

# Mixed-pairing superconductivity in 5d Mott insulators with antisymmetric exchange

Mohammad-Hossein Zare<sup>1,2,\*</sup>, Mehdi Biderang<sup>3,4</sup>, and Alireza Akbari<sup>3,5,6†</sup>

<sup>1</sup>*Department of Physics, Faculty of Science, Qom University of Technology, Qom 37181-46645, Iran*

<sup>2</sup>*School of Mathematics and Physics, University of Queensland, Brisbane, 4072 Queensland, Australia*

<sup>3</sup>*Asia Pacific Center for Theoretical Physics, Pohang, Gyeongbuk 790-784, Korea*

<sup>4</sup>*Department of Physics, University of Isfahan, Hezar Jerib, 81746-73441, Isfahan, Iran*

<sup>5</sup>*Department of Physics, POSTECH, Pohang, Gyeongbuk 790-784, Korea and*

<sup>6</sup>*Max Planck POSTECH Center for Complex Phase Materials, POSTECH, Pohang 790-784, Korea*

(Dated: October 24, 2021)

We investigate the potential existence of a superconducting phase in 5d Mott insulators with an eye to hole doped Sr<sub>2</sub>IrO<sub>4</sub>. Using a mean-field method, a mixed singlet-triplet superconductivity,  $d + p$ , is observed due to the antisymmetric exchange originating from a quasi-spin-orbit-coupling. Our calculation on ribbon geometry shows possible existence of the topologically protected edge states, because of nodal structure of the superconducting gap. These edge modes are spin polarized and emerge as zero-energy flat bands, supporting a symmetry protected Majorana states, verified by evaluation of winding number and  $\mathbb{Z}_2$  topological invariant. At the end, a possible experimental approach for observation of these edge states and determination of the superconducting gap symmetry are discussed based on the quasi-particle interference (QPI) technique.

*Introduction:* Topological superconductors are one of the most outstanding topics in condensed matter because of inevitably hosting Majorana fermions [1]. In contrast to artificial compounds based on the proximity effect [2], class of intrinsic topological superconductor may be realised in heavy fermion noncentrosymmetric superconductors [3] or transition metals oxides (TMOs) [4]. Strong correlated interactions [5, 6] make TMOs into a veritable playground for the study of novel exotic phases. These include intriguing phenomena such as high-temperature superconductivity (SC) in cuprates, colossal magnetoresistance, multi-ferroics, and different ordered magnetic phases [7–10]. This group of materials, especially the 3d-TMOs [11], are ideal systems for observing signatures of Mott insulating behaviour. Recently, a new class of Mott insulators based on iridates, have attracted immense attentions [12–16]. The belief that their Mott phase is motivated by the interplay of electron-electron and spin-orbit coupling (SOC). In these materials, 5d orbitals are partially filled, and because of the extended nature of the 5d orbital, the electron-electron interaction is much smaller than that of 3d Mott insulators. However, the former shows a much larger SOC due to the fact that the strength of the SOC is controlled by the fourth power of the atomic number. Therefore, the intermediate interaction strength together with relatively large SOC makes them a unique and subtle system to study both theoretically and experimentally.

Among the 5d TMOs, the Iridates and specially Sr<sub>2</sub>IrO<sub>4</sub> is widely investigated for superconducting properties. This follows from the structural and electronic similarities with La<sub>2</sub>CuO<sub>4</sub> and Sr<sub>2</sub>RuO<sub>4</sub> [17–19]. In this context, predictions of SC in Sr<sub>2</sub>IrO<sub>4</sub> arise from variational Monte Carlo simulations (VMC) [20], the singular-mode functional renormalization group (SM-FRG)[21], and dynamical mean field theory (DMFT) [22]. However, the nature of the achievable SC is still under de-

bate. While VMC proposes a  $d$ -wave superconducting phase only for electron doping, SM-FRG addresses two possible scenarios: a mixed singlet-triplet SC with  $d_{x^2-y^2}^*$  symmetry for electron doped and a mixed singlet-triplet SC with  $s_{\pm}^*$  symmetry for the hole doped cases. In addition to these methods, DMFT foresees a topological  $p + ip$  pseudo-spin (singlet  $d$ -wave) pairing for hole (electron) doped samples. From experimental point of view, the existence of Fermi arcs suggests electron doped as a potential candidate for the  $d$ -wave SC but with  $T_c$  lower than that of La<sub>2</sub>CuO<sub>4</sub> [23, 24]. Furthermore, a signature of high  $T_c$  is found in electron doping [25] and a  $p$ -wave pairing state is reported by substitution of Ru (hole-doping) [26].

In this paper, by applying a mean-field (MF) approach, we sketch the symmetry and structure of the anomalous order parameter (OP) in the iridates alluded to above. We mainly focus on the broken inversion symmetry, which gives rise to a mixed singlet-triplet superconducting state to arise. This broken inversion symmetry, occurring as a result of the bond-deviations, introduces the antisymmetric exchange and a quasi-SOC (spin-dependent hopping). In particular, we deal with interesting questions such as at what level of the doping or at what strength of the quasi-SOC, SC is recognized in the system, what is the symmetry of the superconducting OP, and more importantly is there a possibility to find a topological SC by calculating the global topological invariants. We believe that our straightforward MF slave boson approach answers these broad questions and opens doors for future analytical and numerical studies.

*Model and Method:* The layered Sr<sub>2</sub>IrO<sub>4</sub> consists of two-dimensional IrO<sub>2</sub> layers, in which Ir<sup>4+</sup> ions form a square lattice. In contrast La<sub>2</sub>CuO<sub>4</sub>, the IrO<sub>6</sub> octahedron in Sr<sub>2</sub>IrO<sub>4</sub> is elongated along the  $c$ -axis and is ro-

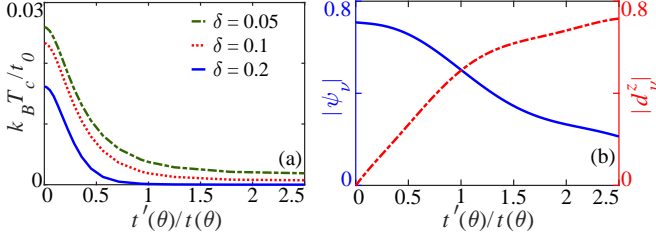


FIG. 1. (Color online) (a) The transition temperature,  $T_c$ , in the mixed singlet-triplet channel versus quasi-SOC (spin-dependent hopping) strength  $t'$  for different doping levels,  $\delta$ . (b) Magnitude of MF order parameters,  $\psi_\nu$  (blue-solid) and  $d_\nu^z$  (dashed-red), plotted as a function  $t'$ , for  $\delta = 0.1$ .

tated around it by an angle  $\theta \approx 11^\circ$  [27]. This deviation angle increases by decreasing of temperature [28]. On top of this, experimental techniques such as X-ray scattering and neutron diffraction indicate a canted antiferromagnetic order in this material [29, 30]. Moreover, the magnetic susceptibility measurement reveals a weak ferromagnetism in  $\text{Sr}_2\text{IrO}_4$  [31]. Due to the strong SOC, the spin and orbital degrees of freedom locally entangle and  $t_{2g}$  orbital splits further into fully filled  $J_{\text{eff}} = 3/2$  (lower), and half-filled  $J_{\text{eff}} = 1/2$  (upper) states. This observation is a result of the reduced energy bandwidth arising from the presence of SOC, which in turn leads to a Mott insulating phase at even smaller  $U$ . The theoretical studies [32, 33] and several experiments [17, 18] support the single orbital picture of the  $J_{\text{eff}} = 1/2$  Mott insulating phase in governing the low energy physics of Ir-oxides [34]. Based on this picture, the single orbital Hubbard model is given by [4, 35, 36]

$$\mathcal{H} = -\sum_{\langle ij \rangle, \alpha} t_0(\theta) c_{i\alpha}^\dagger c_{j\alpha} - \sum_{\langle ij \rangle, \alpha\beta} i(-1)^i t'_0(\theta) c_{i\alpha}^\dagger \sigma_{\alpha\beta}^z c_{j\beta} + \sum_i U n_{i\uparrow} n_{i\downarrow}. \quad (1)$$

Where  $t_0(\theta) = 2t_0/3 \cos\theta(2\cos^4\theta - 1)$ , and  $t'_0(\theta) = 2t_0/3 \sin\theta(2\sin^4\theta - 1)$  are the hopping integrals [36], and  $\sigma$  is the vector of Pauli matrices acting on pseudo-spin space,  $c_{i\alpha}^\dagger$  ( $c_{i\alpha}$ ) stands for the creation (annihilation) operator of an electron with pseudo-spin  $\alpha = \uparrow, \downarrow$  on site  $i$ , and  $n_{i\alpha} = c_{i\alpha}^\dagger c_{i\alpha}$  is a number operator. Here  $U$  is on-site Coulomb interaction, and the first two terms represent effective hopping integrals. The second term is a quasi-SOC and its spin-dependency is formulated from bonding deviation angle,  $\theta$ , from  $180^\circ$  along the Ir-O-Ir bond angle, and behaves in a similar way as an intrinsic SOC. This bond angle can be controlled by tuning the chemical potential,  $\mu$ , or by applying a magnetic field [37] or a strain [38, 39]. At half-filling the effective Hamiltonian may be considered as follows [33, 37],

$$\mathcal{H}_J = \sum_{\langle ij \rangle} \left[ J_H (\mathbf{S}_i \cdot \mathbf{S}_j - \frac{n_i n_j}{4}) + J_z S_i^z S_j^z + \mathbf{D} \cdot \mathbf{S}_i \times \mathbf{S}_j \right], \quad (2)$$

with antiferromagnetic Heisenberg exchange interaction  $J_H$ , the Ising-like exchange interaction  $J_z$ , as well as the antisymmetric Dzyaloshinskii-Moriya (DM) exchange interaction perpendicular to  $\text{IrO}_2$  layers. The latter two terms in the effective exchange Hamiltonian are originated from the quasi-SOC term. Here  $J_H = 4[t_0(\theta)^2 - t'_0(\theta)^2]/U$ ,  $J_z = 8t'_0(\theta)^2/U$ , and  $\mathbf{D} = -D\hat{\mathbf{z}}$  with  $D = 8t_0(\theta)t'_0(\theta)/U$ . Doping introduces itinerant fermionic feature of the system, and in a similar way as cuprates the possible SC can be appeared. To study the superconducting transition temperature,  $T_c$ , and also the symmetry of the anomalous pairing function, we start from the  $t$ - $t'$ - $J$  model as  $\mathcal{H}_{tt'J} = \mathcal{H}_t + \mathcal{H}_{t'} + \mathcal{H}_J$ . Then, we rewrite the pseudo-spin operators in  $\mathcal{H}_J$  as a bilinear of two fermion operators,  $\mathbf{S}_i = \frac{1}{2} f_{i,\alpha}^\dagger \boldsymbol{\sigma}_{\alpha\beta} f_{i,\beta}$ , where  $f_{i\alpha}^\dagger$  is the fermionic spinon creation operator [40]. Substituting the pseudo-spin operators by the fermionic operators, and rephrasing the result in terms of spin singlet and triplet operators:  $s_{ij} = (f_{i\uparrow} f_{j\downarrow} - f_{i\downarrow} f_{j\uparrow})/\sqrt{2}$ ,  $t_{ij,x} = (f_{i\downarrow} f_{j\downarrow} - f_{i\uparrow} f_{j\uparrow})/\sqrt{2}$ ,  $t_{ij,y} = i(f_{i\uparrow} f_{j\uparrow} + f_{i\downarrow} f_{j\downarrow})/\sqrt{2}$ ,  $t_{ij,z} = i(f_{i\uparrow} f_{j\downarrow} + f_{i\downarrow} f_{j\uparrow})/\sqrt{2}$ , the effective Hamiltonian can be reconstructed as

$$\mathcal{H}_J = -\sum_{\langle ij \rangle} \left[ J_H s_{ij}^\dagger s_{ij} + \frac{D}{2} (s_{ij}^\dagger t_{ij,z} + t_{ij,z}^\dagger s_{ij}) + \frac{J_z}{4} (s_{ij}^\dagger s_{ij} - t_{ij,x}^\dagger t_{ij,x} - t_{ij,y}^\dagger t_{ij,y} + t_{ij,z}^\dagger t_{ij,z}) \right]. \quad (3)$$

Therefore, the MF Hamiltonian can be achieved by adopting the spin-singlet and spin-triplet MF OPs:  $\psi_\nu = \langle s_{ij} \rangle/\sqrt{2}$  and  $d_\nu^\gamma = \langle t_{ij,\gamma} \rangle/\sqrt{2}$ . In which,  $\nu \in \{x, y\}$  indicates the direction of the bonds on the square lattice, and  $\gamma$  characterizes the component of the pairing triplet vector. Note that we use the Kotliar-Ruckenstein slave-boson formalism [41] to ensure the Gutzwiller projection. In this formalism, the original electrons are replaced with four auxiliary bosons and one spinful fermion, that at half filling the doublon fields cannot be created at any doping levels. Thus, in MF hopping integrals are renormalized by factor of  $\eta = 2\delta/(1+\delta)$  that  $\delta$  determines the hole doping values, and shows itself in the Hamiltonian by marking  $t = t(\theta) = \eta t_0(\theta)$ , and  $t' = t'(\theta) = \eta t'_0(\theta)$ . Finally, by Fourier transformation (FT) of the fermionic operators, the total MF Hamiltonian can be written as,

$$\mathcal{H}_{MF} = \sum_{\mathbf{k}\alpha\beta} (\varepsilon_{\mathbf{k}} + \mathbf{g}_{\mathbf{k}} \cdot \boldsymbol{\sigma})_{\alpha\beta} f_{\mathbf{k}\alpha}^\dagger f_{\mathbf{k}\beta} + (\Delta_{\mathbf{k}}^{\alpha\beta} f_{\mathbf{k}\alpha}^\dagger f_{-\mathbf{k}\beta}^\dagger + h.c.), \quad (4)$$

where the dispersion is defined by  $\varepsilon_{\mathbf{k}} = -2t(\theta)(\cos k_x + \cos k_y) - \mu$ , and the Rashba type term,  $\mathbf{g}_{\mathbf{k}} = -2t'(\theta)(\sin k_x + \sin k_y)\hat{\mathbf{z}}$ , is originated from the quasi-SOC. Because of a rotation of the oxygen octahedra, the inversion symmetry is locally broken and a DM interaction allows for the non-cubic structures like  $\text{Sr}_2\text{IrO}_4$ . As a result, the spin singlet and triplet pairings coincide in the gap function, i.e.,  $\Delta_{\mathbf{k}} = i(\psi_{\mathbf{k}} \sigma_0 + \mathbf{d}_{\mathbf{k}} \cdot \boldsymbol{\sigma}) \sigma_y$ , and their contributions are accessed via  $\psi_{\mathbf{k}} = 1/4 \sum_\nu [(4J_H +$

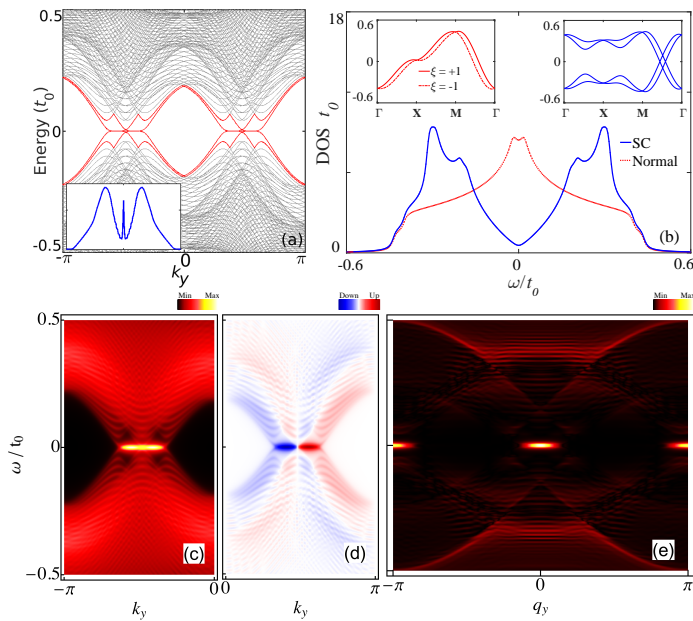


FIG. 2. (Color online) (a) The Bogoliubov electronic dispersion of hole doped  $\text{Sr}_2\text{IrO}_4$  on a ribbon for the topological phase; the red bands indicate the topological in-gap edge states with two-fold degenerate zero-energy Majorana-type with flat bands. Inset represents the edge LDOS of the superconducting state, where the zero energy pick is originated from the zero-energy flat bands, the range of the plot is the same as (b). (b) Bulk LDOS in normal (red-dashed) and superconducting (blue-solid) phases. Insets: left shows the band structure of quasi-spin-orbit split bands:  $\xi = \pm 1$ , in normal phase, and right presents the quasi-particle bands in superconducting phase. (c,d) The intensity plots of the momentum- and spin-resolved LDOS along the  $\Gamma$ -Y momentum direction, respectively. The up and down helical states in (d) correspond to the states with the winding numbers  $+1$  and  $-1$ , respectively. (e) Intensity of the QPI dispersion (absolute value) at the edge (slab:  $n = 1$ ) for the  $Y'$ - $\Gamma$ - $Y$  momentum direction.

$J_z \cos k_y \psi_\nu + 2D \cos k_y d_\nu^z$ ,  $d_{\mathbf{k}}^x = -iJ_z/4 \sum_\nu \sin k_\nu d_\nu^x$ ,  $d_{\mathbf{k}}^y = iJ_z/4 \sum_\nu \sin k_\nu d_\nu^y$ , and  $d_{\mathbf{k}}^z = 1/4 \sum_\nu [2D \sin k_\nu \psi_\nu + J_z \sin k_\nu d_\nu^z]$ . Close to  $T_c$  the MF parameters,  $\psi_\nu$  and  $d_\nu^y$ , are suppressed. In order to find  $T_c$ , it is necessary to obtain the eigenvalues of stability matrices for the spin-singlet and spin-triplet OPs, where the critical temperature is determined by finding the largest temperature that at least one of the eigenvalues of different channels be one [42, 43].

In presence of the DM term, the spin-singlet and  $z$ -component of spin-triplet OPs are coupled, while in-plane terms remain untouched. Therefore, the latter terms,  $d_\nu^x$  and  $d_\nu^y$ , have similar stability matrices as well as the set of eigenvalues with two-fold degeneracies. Comparing the critical temperature of the mixed singlet-triplet and the in-plane triplet channels, supports an admixture state of a  $d$ -wave state  $d_{x^2-y^2}$  (nodal) and a  $p$ -wave state  $p_{x-y}^z$ . This is originated from the fact that the spin-triplet component should be aligned

to quasi-SOC direction,  $\mathbf{d}_{\mathbf{k}} \parallel \mathbf{g}_{\mathbf{k}}$ , by its similarity to pure intrinsic SOC [44]. It should be noted that this admixture state is invariant under the time-reversal symmetry. Fig. 1(a) shows the critical temperature of the state as a function of  $t'$  for different doping levels, we set the Coulomb interaction  $U \sim 6t_0$  [20]. To investigate the importance of spin-dependent hopping term in creating the admixture state, the magnitude of the MF parameters,  $\psi_\nu$  and  $d_\nu^z$ , versus  $t'$  are shown in Fig. 1(b). They represent that at  $t' = 0$ , OP is pure singlet, however its triplet part starts to grow by increasing of the quasi-SOC, while simultaneously the singlet part begins to decrease. It should be emphasized that the existence of the mixed superconducting phase can support Majorana edge-modes by closing the bulk SC gap. These topological edge-modes can be characterized via calculating the momentum dependent winding number for the edge states, which shows changes as a result of projection of the bulk-gap nodes [45–47].

*Topological invariants:* To study the edge modes of superconducting state, we consider the system as a ribbon with open and periodic boundary conditions along  $x$ - and  $y$ -directions, respectively. Employing the ‘‘Altland and Zirnbauer ten-fold’’ classification [48, 49] puts the Hamiltonian (Eq. 4) in the ‘‘class DIII’’, with the ‘‘global  $\mathbb{Z}_2 = 1$  topological number’’. The energy spectrum of the admixture SC, versus the momentum  $k_y$  for  $\theta = 11^\circ$  is shown in Fig. 2(a), while the red lines indicate the degenerate edge states. Here and in the rest of the paper, we fix  $\delta = 0.1$  ( $\mu = -0.02t_0$ ) corresponding to deviation angle  $\theta = 11^\circ$ , thus  $\psi_x = -\psi_y = 0.7$ ,  $d_x^z = -d_y^z = -0.12$ , and since the mixed superconducting phase is stable the remaining MF parameters are zero. In the insets of Fig. 2(b), we show the band structure of quasi-spin-orbit split bands:  $\xi = \pm 1$ , in normal phase (left panel), and the quasi-particle bands in superconducting phase (right panel). The bulk density of states (LDOS) in normal (dashed line) and superconducting (solid line) phases are presented in Fig. 2(b). To investigate the topological nature of SC phase, we calculate the momentum- and spin-resolved LDOS in Fig. 2(c&d), respectively. In particular, the polarization of spin-resolved LDOS shows strong momentum dependency and its sign tendency at each flat bands can be interpreted as changing of winding number,  $W = \pm 1$ , for corresponding bands. As it is shown in the right inset of Fig. 2(a), these protected states lead to finite density of states at zero energy, which can be detected as a zero bias hump in the  $dI/dV$  curve of scanning tunneling microscopy (STM) at the edge of the sample. The general form of the finding results are qualitative the same by changing the deviation angle, before the SC becomes unstable for the larger angles.

*Quasiparticle interference (QPI):* The STM-based

QPI is one of the remarkable techniques to picture the possible existence of a superconducting state and investigating its pairing symmetry. It can show information on the gap symmetry in connection with its dependency on the phase of the superconducting OPs and also on the form and change of the constant energy contours [50]. Here, we provide an innovative way to probe the zero-energy nontrivial modes using QPI. For this purpose, the system is divided into parallel lines ( $n=1, 2, \dots, N$ ) along  $y$ -direction, which contains the nodes of the superconducting gap. Therefore, the Bogoliubov-de Gennes (BdG) Hamiltonian is expressed as  $\mathcal{H}_{BdG} = \frac{1}{2} \sum_{k_y} \Psi_{k_y}^\dagger \mathcal{H}_{k_y} \Psi_{k_y}$ , in which  $\Psi_{k_y}^\dagger = (\Phi_{1,k_y}^\dagger, \Phi_{2,k_y}^\dagger, \dots, \Phi_{N,k_y}^\dagger)$  is the generalized Nambu basis with  $\Phi_{n,k_y}^\dagger = (f_{n,k_y,\uparrow}^\dagger, f_{n,k_y,\downarrow}^\dagger, f_{n,-k_y,\uparrow}, f_{n,-k_y,\downarrow})$ . Then, the recursive relation for describing the superconducting slabs in the basis of Nambu spinors,  $4 \times 4$  matrix representation, is followed by

$$T\Phi_{n-1,k_y} + M\Phi_{n,k_y} + T^\dagger\Phi_{n+1,k_y} = \zeta\Phi_{n,k_y},$$

with the boundary condition:  $\Phi_{0,k_y} = \Phi_{N+1,k_y} = 0$ . Here,  $\zeta$  represents the eigenvalue matrix of the  $\mathcal{H}_{BdG}$  whose eigenstates decay exponentially along  $x$ .  $T$  defines the hopping matrix connecting the nearest-neighbor slabs, and  $M$  encodes the intra-hopping between degrees of freedom inside each slab as well as on-site energies:

$$\begin{aligned} M &= -(2t \cos k_y + \mu)\vartheta_{z0} + [\psi_y D + \frac{d_y^z}{2}] \sin k_y \vartheta_{xz} \\ &\quad - [\psi_y (2J + \frac{J_z}{2}) + d_y^z] \cos k_y \vartheta_{yy} - 2t' \cos k_y \vartheta_{0z}, \\ T &= -t\vartheta_{z0} - it'\vartheta_{0z} - (D + \frac{J_z}{2})(i\vartheta_{xx} + \vartheta_{yy}) - 2J\vartheta_{yy}, \end{aligned}$$

here  $\vartheta_{\alpha\beta} = \tau_\alpha \otimes \sigma_\beta$ , and  $\tau_\alpha$  are Pauli's matrices acting on particle-hole space. The practical way to determine QPI is to find FT of spatial modulation of STM data due to the elastic scattering of quasiparticles from impurity potential,  $V$ , which in the full Born approximation is proportional to changes in local density of states, given by

$$\delta N(q_y, \omega) = -\frac{1}{\pi} V \text{Im} \left[ \Lambda(q_y, i\omega) \right]_{i\omega \rightarrow \omega + i0^+}. \quad (5)$$

Hence, QPI intensity for the  $s^{\text{th}}$  slab, using the t-matrix formalism as outlined in Refs. [51, 52], is obtained as

$$\Lambda_s(q_y, i\omega) = \sum_{k_y} \text{Tr}_\sigma \left[ P_\tau \hat{\rho} \hat{G}(k_y, i\omega) \hat{\rho} \hat{G}^\dagger(k_y - q_y, i\omega) \right]_s,$$

where index  $s$  indicates the tracing over the elements in individual block matrix of the slab  $s$ . Here the projector  $P_\tau = I \otimes (\vartheta_{00} + \vartheta_{z0})/2$  and interaction  $\hat{\rho} = I \otimes \vartheta_{z0}$  act on the generalised Nambu space, in which  $I$  is an identity matrix of size  $N$ . Moreover, the retarded Green's function  $\hat{G}(k_y, i\omega) = (i\omega - \mathcal{H}_{k_y})^{-1}$  is defined for full slab

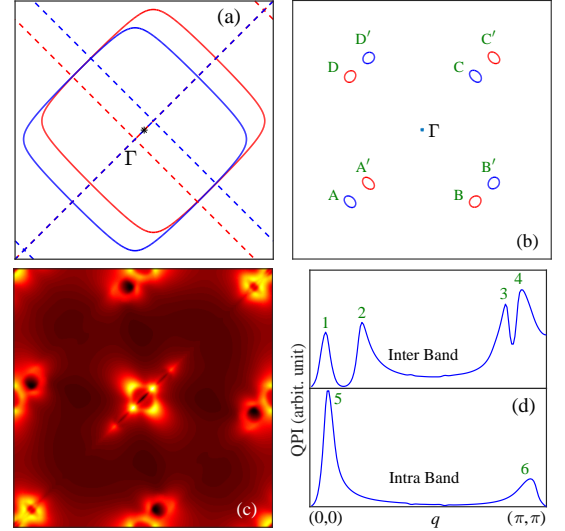


FIG. 3. (Color online) (a) Fermi surface energy contours (solid lines): blue (red) represents the band with  $\xi = -1$  ( $\xi = +1$ ); the dashed lines indicate the node structure of the gap function. (b) Constant contours of energy (spectral function) for the superconducting state, in  $(k_x, k_y)$ -plane at  $\omega = 0.1t_0$ . The small pockets, A, A', ..., appear around the nodes in the spectral function, moderate the scattering wave vectors. (c) The absolute value of the total QPI spectrum in  $(q_x, q_y)$ -plane, corresponding to spectral function in (b). Note: plots range in a-c are  $[-\pi, \pi]$ . (d) The QPI intensity along the  $(0, 0) - (\pi, \pi)$  direction, for inter- (intra-) band scattering in upper (lower) panel. The peaks (1–6) are related to the main scattering vectors, namely 1&2: BB', DD', 3&4: A'C & AC', 5: BB & B'B' (DD & D'D'), and 6: AC & A'C'.

geometry. The results of the intensity plots for the spectral function dispersion and the corresponding QPI dispersion for the edge state (slab:  $n = 1$ ) are shown in the Fig. 2(c-f). Indeed the edge state modes can easily be seen as zero-energy flat bands in both spectral functions (momentum and spin-resolved LDOS) in Fig. 2(c&d), as well as, the QPI dispersions in Fig. 2(e). These flat dispersion bands are absent for the bulk state (middle slab). We note that, to detect these edge states experimentally, one should measure the QPI in  $[100]$ -plane, since there is no dispersion along the  $k_z$  direction.

Finally, to explore the nodal structure of the suggested superconducting state, the QPI spectrum has been presented in the  $xy$ -plane (bulk QPI), which comes by [51]

$$\begin{aligned} \Lambda(\mathbf{q}, i\omega_n) &= \frac{1}{4N} \sum_{\mathbf{k}\xi\xi'} (1 + \xi\xi' \hat{\mathbf{g}}_{\mathbf{k}} \cdot \hat{\mathbf{g}}_{\mathbf{k}-\mathbf{q}}) \times \\ &\quad \frac{(i\omega_n + \epsilon_{\mathbf{k}\xi})(i\omega_n + \epsilon_{\mathbf{k}-\mathbf{q}\xi'}) - \Delta_{\mathbf{k}\xi} \Delta_{\mathbf{k}-\mathbf{q}\xi'}}{[(i\omega_n)^2 - E_{\mathbf{k}\xi}^2][(i\omega_n)^2 - E_{\mathbf{k}-\mathbf{q}\xi'}^2]}, \end{aligned}$$

where the effective quasiparticle energies,  $E_{\mathbf{k}\xi} = \sqrt{\epsilon_{\mathbf{k}\xi}^2 + \Delta_{\mathbf{k}\xi}^2}$ , related to the quasi-spin-orbit split-dispersions ( $\xi = \pm 1$ ) defined by  $\epsilon_{\mathbf{k}\xi} = \epsilon_{\mathbf{k}} + \xi |\mathbf{g}_{\mathbf{k}}|$  with superconducting gap  $\Delta_{\mathbf{k}\xi} = \psi_{\mathbf{k}} + \xi d_{\mathbf{k}}^z$ . We present in

the Fig. 3(a) the normal state electron Fermi surface, where the gap zeroes are displayed as dashed lines, and the resulting split bands:  $\xi = -1$  (blue), and  $\xi = +1$  (red) are shown in the insets of Fig. 2(b). The contours of the quasiparticle energies,  $E_{\mathbf{k}\xi}$ , at constant energy  $\omega = 0.1t_0$ , are schemed in Fig. 3(b). The small pockets, appear around the nodes in the spectral function, lead the scattering wave vectors that play the main role in QPI pattern as shown in Fig. 3(c). To better tracing of the scattering vectors, we show the QPI intensity along the  $(0,0) - (\pi,\pi)$  direction, for both inter- and intra-band scatterings process in Fig. 3(d).

*Summary:* By focusing on hole doped  $\text{Sr}_2\text{IrO}_4$ , we predict that the mixed singlet-triplet superconductivity can exist in layered  $5d$  transition metal oxides, as an example of the new class Mott insulators. Our results demonstrates that the Dzyaloshinskii-Moriya interaction plays an important role in finding this interesting novel phase by preserving the time-reversal symmetry. This also conjectures the existence of a mixed-paring phase, boosted by antisymmetric exchange, in other iridates that host a similar mechanism for an insulating state. This insulating state is confirmed for other iridates such as  $\text{Sr}_3\text{Ir}_2\text{O}_7$  [53, 54] and  $\text{BaIrO}_3$  [55]. This analysis can be extended to models, which also include the second-neighbour and the third-neighbour Heisenberg coupling. Together with this prediction, we present a possible method for experimentally observing the zero-energy nontrivial edge states by STM-based QPI approach.

*Acknowledgments:* We would like to thank G. Khalullin, B.J. Kim, A. Schnyder, P. Thalmeier, P. Fulde, R. H. McKenzie, A. R. Wright, M. Kargarian, A.G. Moghaddam, J. Yu, and E. Taghizadeh, for useful discussions. M.H.Z thanks Asia Pacific Center for Theoretical Physics (APCTP) for hospitality. A.A. acknowledges support through NRF funded by MSIP of Korea (2015R1C1A1A01052411), and by Max Planck POSTECH / KOREA Research Initiative (No. 2011-0031558) programs through NRF funded by MSIP of Korea.

---

\* zare@qut.ac.ir

† alireza@apctp.org

- [1] C. W. J. Beenakker, Rev. Mod. Phys. **87**, 1037 (2015).
- [2] S. Nadj-Perge, I. K. Drozdov, J. Li, H. Chen, S. Jeon, J. Seo, A. H. MacDonald, B. A. Bernevig, and A. Yazdani, Science **346**, 602 (2014).
- [3] M. Sato and S. Fujimoto, Phys. Rev. B **79**, 094504 (2009).
- [4] J. G. Rau, E. K.-H. Lee, and H.-Y. Kee, Annual Review of Condensed Matter Physics **7**, 195 (2016).
- [5] M. Imada, A. Fujimori, and Y. Tokura, Rev. Mod. Phys. **70**, 1039 (1998).
- [6] B. H. Brandow, Advances In Physics **26**, 651 (1977).
- [7] Y. Tokura and N. Nagaosa, Science **288**, 462 (2000).
- [8] E. Dagotto, Science **309**, 257 (2005).
- [9] P. A. Lee, N. Nagaosa, and X.-G. Wen, Rev. Mod. Phys. **78**, 17 (2006).
- [10] D. J. Scalapino, Rev. Mod. Phys. **84**, 1383 (2012).
- [11] J. Zaanen, G. A. Sawatzky, and J. W. Allen, Phys. Rev. Lett. **55**, 418 (1985).
- [12] W. Witczak-Krempa, G. Chen, Y. B. Kim, and L. Balents, Annu. Rev. Condens. Matter Phys. **5**, 57 (2014).
- [13] R. J. Cava, B. Batlogg, K. Kiyono, H. Takagi, J. J. Krajewski, W. F. Peck, L. W. Rupp, and C. H. Chen, Phys. Rev. B **49**, 11890 (1994).
- [14] T. Shimura, Y. Inaguma, T. Nakamura, M. Itoh, and Y. Morii, Phys. Rev. B **52**, 9143 (1995).
- [15] S. J. Moon, H. Jin, K. W. Kim, W. S. Choi, Y. S. Lee, J. Yu, G. Cao, A. Sumi, H. Funakubo, C. Bernhard, and T. W. Noh, Phys. Rev. Lett. **101**, 226402 (2008).
- [16] G. Cao and P. Schlottmann, ArXiv e-prints (2017), arXiv:1704.06007 [cond-mat.str-el].
- [17] J. Kim, D. Casa, M. H. Upton, T. Gog, Y.-J. Kim, J. F. Mitchell, M. van Veenendaal, M. Daghofer, J. van den Brink, G. Khaliullin, and B. J. Kim, Phys. Rev. Lett. **108**, 177003 (2012).
- [18] S. Fujiyama, H. Ohsumi, T. Komesu, J. Matsuno, B. J. Kim, M. Takata, T. Arima, and H. Takagi, Phys. Rev. Lett. **108**, 247212 (2012).
- [19] M. F. Ceting, P. Lemmens, V. Gnezdilov, D. Wulferding, D. Menzel, T. Takayama, K. Ohashi, and H. Takagi, Phys. Rev. B **85**, 195148 (2012).
- [20] H. Watanabe, T. Shirakawa, and S. Yunoki, Phys. Rev. Lett. **110**, 027002 (2013).
- [21] Y. Yang, W.-S. Wang, J.-G. Liu, H. Chen, J.-H. Dai, and Q.-H. Wang, Phys. Rev. B **89**, 094518 (2014).
- [22] Z. Y. Meng, Y. B. Kim, and H.-Y. Kee, Phys. Rev. Lett. **113**, 177003 (2014).
- [23] Y. K. Kim, O. Krupin, J. D. Denlinger, A. Bostwick, E. Rotenberg, Q. Zhao, J. F. Mitchell, J. W. Allen, and B. J. Kim, Science **345**, 187 (2014).
- [24] Y. K. Kim, N. H. Sung, J. D. Denlinger, and B. J. Kim, Nat Phys **12**, 37 (2016).
- [25] Y. J. Yan, M. Q. Ren, H. C. Xu, B. P. Xie, R. Tao, H. Y. Choi, N. Lee, Y. J. Choi, T. Zhang, and D. L. Feng, Phys. Rev. X **5**, 041018 (2015).
- [26] S. J. Yuan, S. Aswartham, J. Terzic, H. Zheng, H. D. Zhao, P. Schlottmann, and G. Cao, Phys. Rev. B **92**, 245103 (2015).
- [27] M. K. Crawford, M. A. Subramanian, R. L. Harlow, J. A. Fernandez-Baca, Z. R. Wang, and D. C. Johnston, Phys. Rev. B **49**, 9198 (1994).
- [28] S. Chikara, O. Korneta, W. P. Crummett, L. E. DeLong, P. Schlottmann, and G. Cao, Journal of Applied Physics **107**, 09D910 (2010).
- [29] S. J. Moon, H. Jin, W. S. Choi, J. S. Lee, S. S. A. Seo, J. Yu, G. Cao, T. W. Noh, and Y. S. Lee, Phys. Rev. B **80**, 195110 (2009).
- [30] F. Ye, S. Chi, B. C. Chakoumakos, J. A. Fernandez-Baca, T. Qi, and G. Cao, Phys. Rev. B **87**, 140406 (2013).
- [31] G. Cao, J. Bolivar, S. McCall, J. E. Crow, and R. P. Guertin, Phys. Rev. B **57**, R11039 (1998).
- [32] H. Watanabe, T. Shirakawa, and S. Yunoki, Phys. Rev. Lett. **105**, 216410 (2010).
- [33] G. Jackeli and G. Khaliullin, Phys. Rev. Lett. **102**,



- 017205 (2009).
- [34] J. W. Kim, Y. Choi, J. Kim, J. F. Mitchell, G. Jackeli, M. Daghofer, J. van den Brink, G. Khaliullin, and B. J. Kim, *Phys. Rev. Lett.* **109**, 037204 (2012).
- [35] F. Wang and T. Senthil, *Phys. Rev. Lett.* **106**, 136402 (2011).
- [36] H. Jin, H. Jeong, T. Ozaki, and J. Yu, *Phys. Rev. B* **80**, 075112 (2009).
- [37] M. Ge, T. F. Qi, O. B. Korneta, D. E. De Long, P. Schlottmann, W. P. Crummett, and G. Cao, *Phys. Rev. B* **84**, 100402 (2011).
- [38] B. Kim, P. Liu, and C. Franchini, *ArXiv e-prints* (2017), arXiv:1701.08942 [cond-mat.str-el].
- [39] J. Nichols, J. Terzic, E. G. Bittle, O. B. Korneta, L. E. D. Long, J. W. Brill, G. Cao, and S. S. A. Seo, *Applied Physics Letters* **102**, 141908 (2013).
- [40] X.-G. Wen, *Phys. Rev. B* **65**, 165113 (2002).
- [41] G. Kotliar and A. E. Ruckenstein, *Phys. Rev. Lett.* **57**, 1362 (1986).
- [42] A. M. Black-Schaffer and S. Doniach, *Phys. Rev. B* **75**, 134512 (2007).
- [43] T. Hyart, A. R. Wright, G. Khaliullin, and B. Rosenow, *Phys. Rev. B* **85**, 140510 (2012).
- [44] P. A. Frigeri, D. F. Agterberg, A. Koga, and M. Sigrist, *Phys. Rev. Lett.* **92**, 097001 (2004).
- [45] M. Sato, Y. Tanaka, K. Yada, and T. Yokoyama, *Phys. Rev. B* **83**, 224511 (2011).
- [46] Y. Tanaka, M. Sato, and N. Nagaosa, *Journal of the Physical Society of Japan* **81**, 011013 (2012).
- [47] A. P. Schnyder, C. Timm, and P. M. R. Brydon, *Phys. Rev. Lett.* **111**, 077001 (2013).
- [48] A. P. Schnyder, S. Ryu, A. Furusaki, and A. W. W. Ludwig, *Phys. Rev. B* **78**, 195125 (2008).
- [49] C.-K. Chiu, J. C. Y. Teo, A. P. Schnyder, and S. Ryu, *Rev. Mod. Phys.* **88**, 035005 (2016).
- [50] D. J. Singh and M.-H. Du, *Phys. Rev. Lett.* **100**, 237003 (2008); J. Knolle, I. Eremin, A. Akbari, and R. Moessner, *Phys. Rev. Lett.* **104**, 257001 (2010); T. Hanaguri, S. Niitaka, K. Kuroki, and H. Takagi, *Science* **328**, 474 (2010); M. P. Allan, A. W. Rost, A. P. Mackenzie, Y. Xie, J. C. Davis, K. Kihou, C. H. Lee, A. Iyo, H. Eisaki, and T.-M. Chuang, *ibid.* **336**, 563 (2012); A. Akbari, P. Thalmeier, and I. Eremin, *Phys. Rev. B* **84**, 134505 (2011); M. P. Allan, F. Masee, D. K. Morr, J. V. Dyke, A. W. Rost, A. P. Mackenzie, C. Petrovic, and J. C. Davis, *Nature Physics* **9**, 468 (2013); B. B. Zhou, S. Misra, E. H. d. S. Neto, P. Aynajian, R. E. Baumbach, J. D. Bauer, E. D. Thompson, and A. Yazdani, *ibid.* **9**, 474 (2013).
- [51] A. Akbari and P. Thalmeier, *Europhysics Letters* **102**, 57008 (2013); *Eur. Phys. J. B* **86**, 495 (2013).
- [52] F. Lambert, A. Akbari, P. Thalmeier, and I. Eremin, *Phys. Rev. Lett.* **118**, 087004 (2017).
- [53] M. Moretti Sala, V. Schnells, S. Boseggia, L. Simonelli, A. Al-Zein, J. G. Vale, L. Paolasini, E. C. Hunter, R. S. Perry, D. Prabhakaran, A. T. Boothroyd, M. Krisch, G. Monaco, H. M. Ronnow, D. F. McMorrow, and F. Mila, *Phys. Rev. B* **92**, 024405 (2015).
- [54] X. Lu, D. E. McNally, M. Moretti Sala, J. Terzic, M. H. Upton, D. Casa, G. Ingold, G. Cao, and T. Schmitt, *Phys. Rev. Lett.* **118**, 027202 (2017).
- [55] M. A. Laguna-Marco, D. Haskel, N. Souza-Neto, J. C. Lang, V. V. Krishnamurthy, S. Chikara, G. Cao, and M. van Veenendaal, *Phys. Rev. Lett.* **105**, 216407 (2010).